Journal of Nuclear Materials 547 (2021) 152761

Contents lists available at ScienceDirect

Journal of Nuclear Materials

journal homepage: www.elsevier.com/locate/jnucmat

Fracture-mechanical properties of neutron irradiated ITER specification tungsten

E. Gaganidze[a,*], A. Chauhan[a], H.-C. Schneider[a], D. Terentyev[b], G. Borghmans[b], J. Aktaa[a]

[a] Karlsruhe Institute of Technology, Institute for Applied Materials (IAM), Hermann-von-Helmholtz-Platz 1, 76344 Eggenstein-Leopoldshafen, Germany
[b] SCK•CEN, Institute of Nuclear Materials Science, Boeretang 200, B2400 Mol, Belgium

ARTICLE INFO

Article history:
Received 10 September 2020
Revised 22 December 2020
Accepted 23 December 2020
Available online 8 January 2021

Keywords:
Polycrystalline tungsten, Fracture behaviour
Neutron irradiation

ABSTRACT

The work focuses on the investigation of the influence of neutron irradiation on the fracture mechanical properties of ITER specification-conform, stress-relieved tungsten bar. The irradiation of miniaturized Three-Point Bend specimens was performed inside the fuel channel of the Material Test High Flux BR2 reactor of SCK•CEN in Mol. An irradiation damage dose close to 1 dpa (in tungsten) was achieved at 800°C with active temperature cooling and constant on-line temperature monitoring. Thick-wall stainless steel capsules were implemented for shielding the thermal neutrons in order to reduce Re transmutation down to ~2 at.% (and 0.2 at.% Os). The quasi-static fracture mechanical experiments were carried out following ASTM E399 aiming at the determination of plane strain fracture toughness K_{Ic}. The post irradiation examination of the specimens irradiated at 800°C reveals severe material embrittlement. At $T_{test} = T_{irr} = 800$°C, a deformation free brittle fracture is observed. The fractographic investigations show a mixture of brittle transgranular cleavage and intergranular fracture. With increasing the test temperature above 1000°C, the fracture mode is changed from the brittle to a ductile one. Blunting of the notch tip leads to a suppression of the crack initiation and propagation and consequently no failure of the specimens was observed up to severe deflection levels. In some cases, however, a ductile crack growth with a characteristic dimple formation was identified, in addition. Based on the obtained results, the Ductile to Brittle Transition Temperature shift induced by the neutron irradiation at 800°C is evaluated to be 600-625°C.

1. Introduction

A DEMOnstration fusion power plant (DEMO) will be the nearest-term fusion reactor demonstrating production of several hundred MWs of net electricity and operating with closed tritium fuel-cycle [1]. The severe operational environment of the first wall and divertor Plasma Facing Components (PFC) of DEMO comprises extremely high fluences from neutral particles together with the energetic ions escaping the plasma. This imposes specific requirements on the candidate Plasma Facing Materials (PFM) of the future fusion reactors [2]. In addition to the plasma particle driven erosion, melting and cracking [2], 14 MeV neutrons will further degrade the mechanical and thermo-physical properties of the PFM by the production of atomic displacement damage as well as solid and gaseous transmutation products [3]. Due to its numerous favourable thermo-physical, mechanical and high heat flux properties, tungsten is currently considered as a baseline armour material for DEMO PFCs [2,4]. However, the inherent low fracture toughness, high ductile-to-brittle-transition temperature (DBTT) [5–9] and low recrystallization temperature [10], determine the limiting factors for the application of tungsten and its alloys. The DBTT of polycrystalline bulk tungsten defines a lower application temperature limit of the material and consequently, the prediction of the component lifetime requires thorough characterization of fracture mechanical properties of the constituent tungsten alloys both in the reference unirradiated state as well as after neutron irradiation in the fusion application relevant temperature range. The fracture behavior of the polycrystalline tungsten products depends strongly on a fabrication route specific anisotropic microstructure, determined by product shape and applied thermo-mechanical treatment [6,8,11]. A relative orientation of the initial crack plane with respect to the product specific grain microstructure is found to play essential role in the fracture behavior. Microstructure of rolled polycrystalline rods is characterized by the existence of the elongated grains parallel to the rolling direction

* Corresponding Author: E. Gaganidze, Karlsruhe Institute of Technology, Institute for Applied Materials (IAM), Hermann-von-Helmholtz-Platz 1, 76344 Eggenstein-Leopoldshafen, Germany.
E-mail address: ermile.gaganidze@kit.edu (E. Gaganidze).

https://doi.org/10.1016/j.jnucmat.2020.152761
0022-3115/

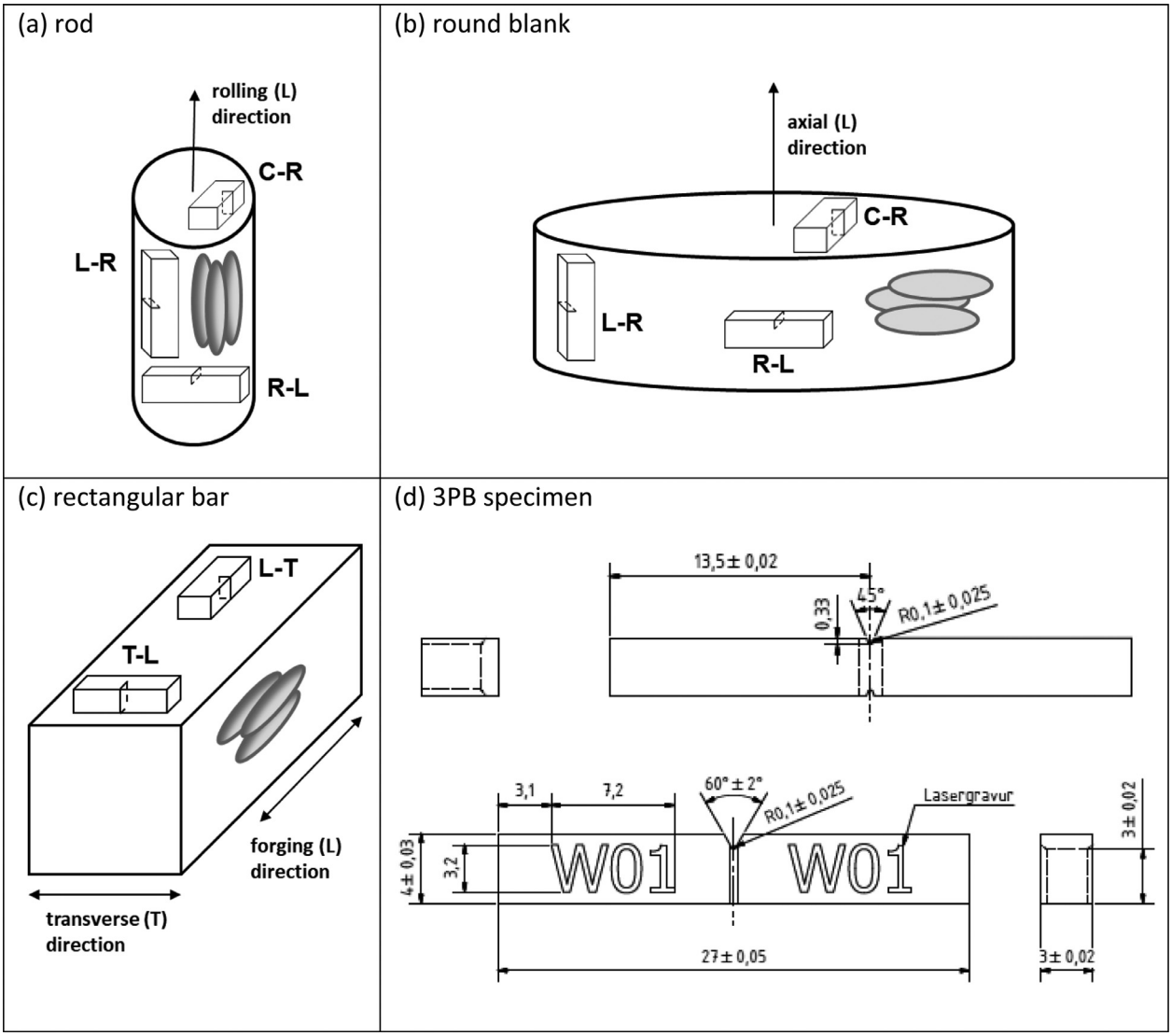

Figure 1. Illustration of specimen machining direction and specimen crack plane orientation for different semi-finished products (a), (b), (c) and specimen technical drawing (d); Grains elongated parallel to rolling direction of a rod and parallel to the forging direction of a bar are schematically indicated in (a) and (c), respectively; Platelet shaped grains parallel of the round blank base are schematically shown in (b); Technical drawing of miniaturized 3PB specimens is shown in (d).

[6]. The C-R and R-L orientation of specimens (see Figure 1 as well as the nomenclature for rod products in ASTM E399 [12]) promoted intergranular crack propagation, whereas, the orientation L-R promoted transgranular cleavage, and thus, lead to larger effective fracture toughness in comparison to C-R and R-L orientations [6]. The microstructure of round blank tungsten products manufactured via sintering into the rods and subsequent forging to the round blanks (deformation degree 80 %) was characterized by the presence of platelet shaped grains being stacked parallel to a base of the round blank [8]. In contrast to the rod material, it was now the L-R orientation which promoted the intergranular fracture [8]. R-L and C-R orientations in contrast promoted transgranular cleavage, thus, leading to effectively higher fracture toughness values. The intergranular fracture was attributed to the presence of trace impurities such as phosphorus at the grain boundaries of the polycrystalline tungsten [13]. Detailed investigation of how representative impurities (P, O, S) affect the fracture behaviour of technically pure (99.97% purity) tungsten and tungsten samples with higher and lower impurity contents was carried out in [14]. In technically pure materials the small amounts of the impurities were reported not to influence the crack path, while other factors e.g. grain microstructure and dislocation density were found to have a stronger influence on fracture mechanisms. A minimum purity level required for ITER is 99.94 wt.% [15]. The influence of the neutron irradiation on the microstructure and hardness of W and W-Re alloys has been extensively studied in, [16–18]. The neutron spectrum of the implemented Material Test Reactor (MTR) was found to play decisive role in the evolution of the irradiation induced defect microstructure [17]. The microstructure developed under irradiation with the fast neutron spectrum at Joyo reactor at around 500°C to ~1 dpa was characterized by the presence of voids (void lattice) and dislocation loops, whereas, no voids were observed after applying mixed spectrum neutron irradiation in the High Flux Isotope Reactor (HFIR). In the latter case, in addition to dislocation loops, the presence of fine scale acicular (χ-phase) precipitates attributed to the formation of transmutation products Re (9.2%) and Os (5%) have been observed. Due to the formation of Re-rich precipitates, a considerably higher increase in Vickers Hardness has been found in the HFIR irradiated specimens, if compared with the Joyo irradiated counterparts [17]. Hu et al. [18] applied dispersed barrier hardening model to correlate neutron irradiation induced microstructural changes to the experimentally determined Vickers

hardness change in pure tungsten after irradiation in HFIR from 90 to 850°C. The voids and TEM-visible dislocation loops were identified as the two major hardening sources after low irradiation doses (<0.3 dpa). At modest doses (>0.6 dpa), however, secondary phase precipitates resulting from the transmutation appeared to dominate radiation induced hardening [18]. The calculation of tungsten transmutation products in [3] showed that 3.8 at.% Re will be produced after 5 years irradiation under first wall fusion power plant conditions which is considerably less than the transmuted Re content after HFIR irradiation in [17]. Consequently, proper control of the nuclear transmutation rates under MTR irradiations is indispensable for a reliable prediction of neutron irradiation effects under fusion environment. The influence of the neutron irradiation on the fracture mechanical properties of the tungsten alloys is rarely reported in the literature. Up to recent, no fracture-mechanical properties were reported in the open literature when it comes to the assessment of the effect of neutron irradiation. Very recently, two studies [19,20] were published to report the effect of neutron irradiation on the fracture toughness of spark plasma sintered tungsten. The authors have reported that the neutron irradiation executed at 600 and 1000 °C at 0.24 dpa leads to the shift of DBTT of 300°C or even larger (the maximum temperature test capacity was 600 °C). In the same works, the authors reported that the hot rolled tungsten (T-L orientation) irradiated at 600 °C becomes brittle as the irradiation dose reaches ~0.7 dpa. The study of the neutron irradiation effects in ITER-specification tungsten irradiated and tested at high temperature (> 600 °C) is currently missing according to author's knowledge. The study of the neutron irradiation effects on the tensile properties of W in strained state as well as after various annealed conditions revealed a profound effect of neutron irradiation on the embrittlement of the material manifested by appearance of brittle failure [21]. A reduction in fracture stress by 5-10 times at T_{test} of ~300 °C has been reported for the strained tungsten after irradiation at 300 °C to about ~10^{21} n/cm^2 neutron fluence. Conversely, irradiation at 500-800°C to ~10^{22} n/cm^2 neutron fluence resulted in appreciable hardening in both strained and annealed conditions [21]. Recently, mechanical properties of commercially available pure tungsten (99.9% purity) have been studied after irradiation with high energy protons and spallation neutrons to doses of 1.3-3.5 dpa and to helium contents of 37-140 appm at 75-110 °C [22]. Here, Three-Point Bend (3PB) tests in the irradiated state revealed brittle fracture without any plastic deformation regardless of the irradiation dose and testing temperature between room temperature (RT) and 500 °C. Fracture mode was found to be of mixed transgranular and intergranular type. In addition, visible slip bands have been observed for a test carried out at 450 °C. The irradiation conditions applied in [22] were tailored for the application of tungsten in spallation targets and are therefore not representative for the operational conditions expected for PFC components of future fusion power plants.

The current work focuses on the investigation of the influence of neutron irradiation under controlled (reduced compared to earlier works done in HFIR) Re production on the fracture mechanical properties of ITER specification-conform, stress-relieved ITER Grade Product (IGP) W bar in the temperature range being relevant for the PFC components. The main emphasis is put on the alteration of the fracture mode after neutron irradiation as well as on the neutron irradiation induced shift in the DBTT. The fracture mechanical properties obtained in the current work will provide significant contribution to the development of EUROfusion materials property handbook for DEMO in-vessel components [23].

2. Experimental

Material studied in the current work is ITER specification-conform, stress-relieved IGP-W bar (36 × 36 × 480 mm^3) of 99.7 wt% purity manufactured by PLANSEE SE, Austria [24]. For the considered purity level the manufacturer specifies the limits of representative impurities C, O, N, Fe, Ni, Si of 30 (6), 20 (2), 5 (1), 30 (8), 20 (2) and 20 (1) µg/g, where the values in parentheses indicate typical maximum values [24]. The mass density at room temperature of 19.25 g/cm^3 [24] also satisfies the lowest limit of 19.0 g/cm^3 of ITER specification [15]. The microstructure of the studied IGP-W bar consists of strongly elongated grains, parallel to the forging direction with a diameter of 5-10 µm and a length of ca. 25 µm, as reported in [25]. Fracture mechanical 3PB specimens of KLST type with the dimensions (B x W x L) of 3 × 4 × 27 mm, and a 1 mm deep V-type notch were machined in T-L orientation, see Figure 1. In order to increase the stress triaxiality, the notch roots fabricated by Electrical Discharge Machining (EDM) were further refined by razor blade polishing according to the procedure described in [11]. The average notch diameter of ca. 66 µm with a standard deviation of 17 µm and the average initial crack length of ca. 1.08 mm were achieved. Finally, side grooves of ca. 0.33 mm depth were introduced leading to a reduction of net specimen thickness B_N down to ca. 2.34 mm. The influence of the used pre-crack type was not studied in the current paper. Comparing the results obtained on the specimens with crack starter notches refined by razor blade polishing method [6] with the results obtained on the specimens involving pre-cracking a chevron-notched specimen in compression and then in tension in [26] shows a reasonably good agreement for measured fracture toughness [6]. The irradiation of miniaturized 3PB specimens was performed inside the fuel channel of the Material Test High Flux BR2 reactor of SCK•CEN in Mol [27]. Damage dose close to 1 dpa (in tungsten, calculated using MCNPX 2.7.0 with JENDL4) has been achieved at 800°C [27]. Stainless steel thick-walled capsules were implemented for shielding from the thermal neutrons to suppress tungsten to rhenium transmutation to a large extent. The total irradiation time was 143 days and the neutron flux was 5 × 10^{14} (E > 0.1 MeV), 2 × 10^{14} (E > 1 MeV) and 4.2 × 10^{14} (E < 0.1 MeV) 1/cm^2/s. The irradiation was performed during 6 cycles in C-type channels (i.e. third raw from the center of the reactor central channel) [27]. The estimated resulted Re content is ~2 at.%, which is still higher than Re content expected after 1 dpa fusion power plant operation (about 0.91 at.% Re will be generated under first wall fusion power plant condition after 1 year according to [3]), however it is still relevant for high dose damage (about 3.8 at % after 5 years [3]). The estimated Os content is 0.2 at.%.

The quasi-static fracture mechanical experiments have been carried out following ASTM E399 standard [12] aiming at the determination of the plane strain fracture toughness K_{Ic} in the frame of linear-elastic fracture mechanics. Contact loads up to 40 N were applied to 3PB specimens prior to displacement-controlled loading at RT or prior starting heating ramp followed by displacement-controlled loading at elevated temperatures. Due to this reason load displacement curves do not start at 0 load in Figure 2. The applied displacement rate of 2 µm/s yielded stress intensity factor rates between 0.6-0.7 MPa•m$^{1/2}$/s. Reference unirradiated W fracture mechanical tests were performed with INSTRON-DOLI universal electro-mechanical testing machines installed in a KIT's cold laboratory and equipped with high temperature vacuum furnaces (up to 1500 °C, typical vacuum 10^{-5} mbar). The testing of irradiated specimens was carried out with servo-electric testing machine Zwick installed in the Hot Cells of Fusion Material Laboratory of KIT. Also, this machine is equipped with a high temperature vacuum furnace (up to 1200°C, typical vacuum 6 × 10^{-5} mbar). For comparison, selected reference tests on the unirradiated specimens have been repeated in the Hot Cells, conforming fairly conditional fracture toughness K_Q values determined according to ASTM E399 in the cold laboratory. A summary of the material states, test tem-

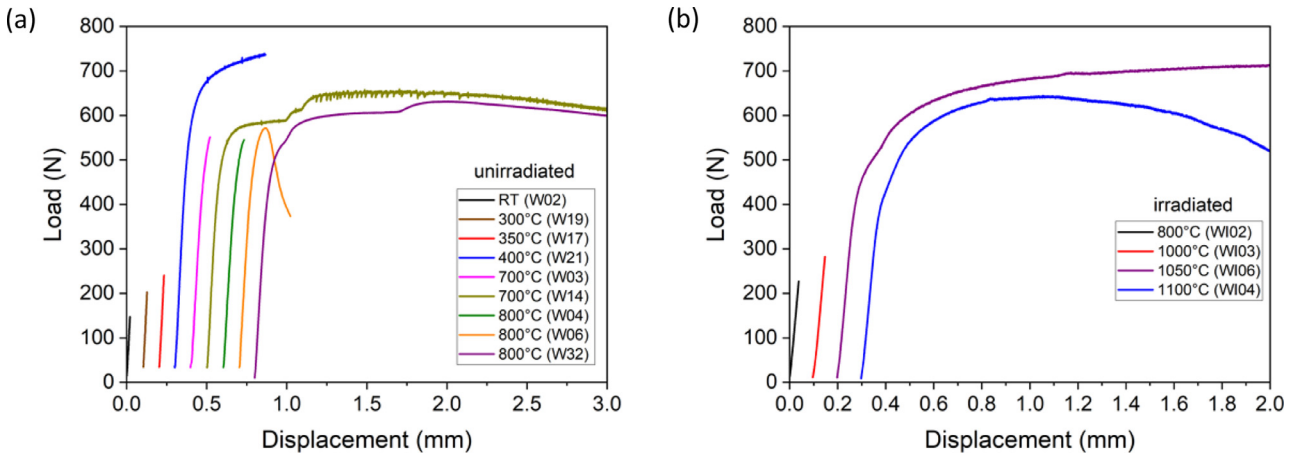

Figure 2. Load vs displacement curves in the unirradiated state (a) and after neutron irradiation to 1 dpa at 800 °C (b). Test temperatures are indicated in the figure legend. For a better appreciation, the curves are shifted on X axis.

Table 1
Material state, test temperature and specimen identification.

State	Unirr.										Irr. (1dpa, 800°C)				
Test T (°C)	25	300	350	400	450	500	600	700	800	1000	800	1000	1025	1050	1100
Specimen	W02	W19, W28	W17	W21, W29	W31	W07	W30	W03, W14, W23, W27	W04, W06, W24, W32	W25, W33	WI02	WI03	WI08	WI06	WI04, WI07

peratures and identification numbers of the specimens are is given in Table 1.

Representative Scanning Electron Microscopy (SEM) investigations have been conducted on selected broken specimens. SEM examination of the fracture surfaces of unirradiated specimens was performed with a Zeiss EVO MA 10 SEM. The examination of fracture surfaces of irradiated specimens have been carried out in the Hot Cells of Fusion Material Laboratory by using an upgraded Cambridge CamScan 44 SEM.

Transmission Electron Microscopy (TEM) examinations of Focused Ion Beam (FIB, FEI Scios) prepared lamellae were performed with a FEI Tecnai G² F20 at 200 kV equipped with a high-angle annular dark-field (HAADF) scanning TEM (STEM) detector.

3. Results

Selected load vs. displacement curves obtained in the reference unirradiated state as well as after neutron irradiation at 800 °C to 1 dpa are shown in Figure 2. In the unirradiated state, the specimens failed in a brittle manner i.e. without deformation at test temperatures up to 350 °C, see Figure 2(a). At a test temperature of 400 °C and above, a non-linear load vs. displacement behavior preceded an abrupt drop of the specimen load. In some cases, however, no failure of the specimens has been observed at elevated temperatures up to large displacements. The latter was limited to about 3 mm by the configuration of the specimen fixtures used. Some examples of variation of load-displacement behavior are shown in Figure 2(a). Testing at 700 °C yielded either to i) brittle fracture just after the onset of nonlinearity (magenta curve) or ii) no failure after achieving relatively large deformation (dark yellow curve). The reason for *staircase* like evolution of load with displacement after initial flattening is not clear. Such behavior was not observed e.g. for polycrystalline round blank tungsten studied in [8]. Comparatively, testing at 800 °C yielded either to i) brittle fracture just after the onset of nonlinearity (green curve), ii) failure after prior stable crack growth (orange curve) or iii) no failure even after achieving relatively large displacement (purple curve). The reason for this qualitatively different high temperature behavior is not clear. Variation of the notch root dimensions and/or shape will lead to different stress triaxialities at the notch roots of investigated specimens, and hence, will affect their deformation behavior. These phenomena need dedicated study in the future. The neutron irradiation at 800 °C to 1 dpa shifted the onset of the non-linear load vs. displacement behavior to higher temperatures, as can be seen from Figure 2(b). At test temperatures below 1000 °C, the brittle fracture takes place within the elastic range of load. The deformation behavior, however, is qualitatively changed after testing the specimens at 1025°C and above it. No fracture of the specimens has been observed up to the achieved displacement. Flattening of the curve at a test temperature of 1050 °C in Figure 2(b) indicates the absence of the crack growth. A slow reduction of the applied load beyond 1 mm displacement for a specimen tested at 1100 °C indicates, in contrast, the initiation and propagation of the crack, supported by the fractographic investigation to be presented later.

Figure 3 shows SEM images of the fracture surface of the unirradiated specimens tested at different temperatures. Brittle fracture, characterized by a mixture of transgranular cleavage and intergranular fracture is observed at test temperatures of 300 and 400 °C in Figure 3(a), (b). Transgranular cleavage propagating through several grains is found to be the dominant fracture mechanism. This fracture behaviour prevented the estimation of the grain size using SEM images directly. In contrast, qualitatively varying fracture behaviour is observed for the specimens tested at 800°C. Some specimens failed in a brittle manner, as shown in Figure 3(c). Evidently, the fracture surface still shows a mixture of transgranular cleavage and intergranular fracture, though the surface morphology became more complex compared to smooth fracture surfaces observed at the lower test temperatures. Furthermore, few locally confined traces of ductile tearing (see marked dotted white arrows in Figure 3(c)) were identified as well. Other specimens, e.g. the one tested at 800 °C shown in Figure 3(d) exhibited ductile crack growth with the characteristic dimple formation. Other tests performed at 700 °C and above were terminated without any recognizable crack growth and therefore without the sample's failure.

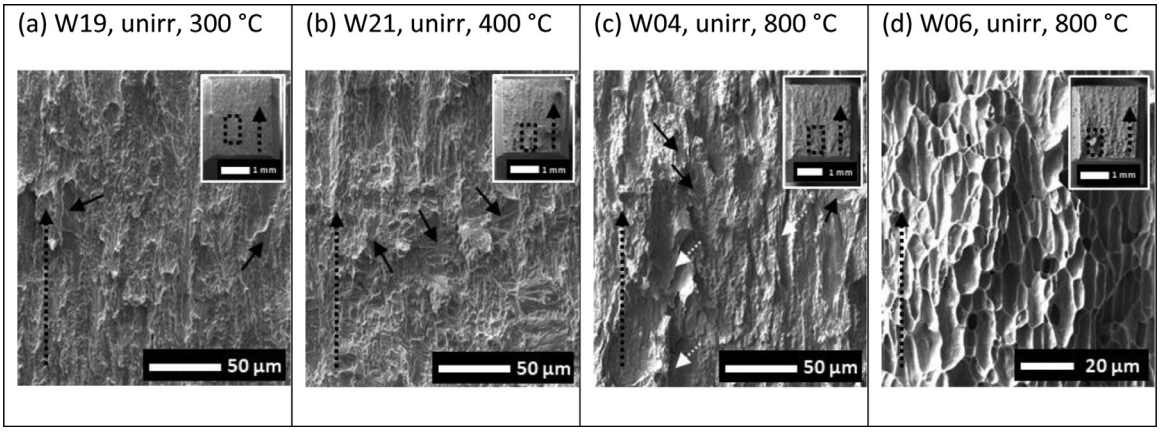

Figure 3. SEM images of the fracture surfaces of unirradiated specimens after testing at different temperatures. Inset shows low magnification fractured specimen images showing marked square region that is enlarged. Crack propagation goes from bottom towards top (see marked black dotted arrows). Transgranular cleavage features are marked by short black arrows in Figures (a-c). Few locally confined traces of ductile tearing are marked by dotted white arrows in (c).

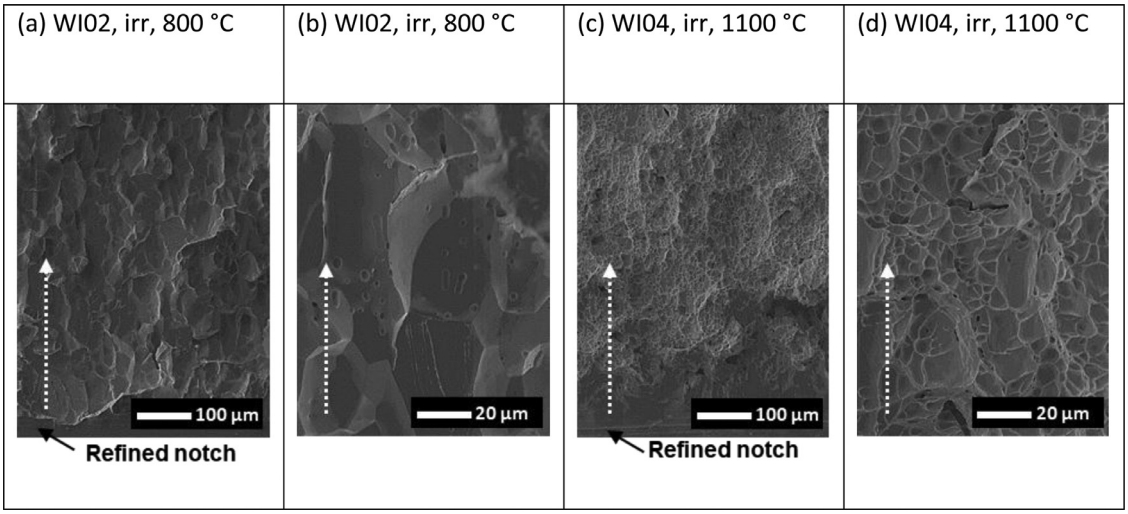

Figure 4. SEM images of fracture surfaces of irradiated specimens after testing at different temperatures. Crack propagation goes from bottom towards top (see marked dotted arrows).

Figure 4 shows fracture surface of the irradiated specimens tested at different temperatures. Brittle fracture is observed for the specimen tested at 800 °C (Figure 4(a), (b)) which failed in the linear elastic regime of the load vs. displacement curve in Figure 2(b). Fracture type is predominantly intergranular as can be seen at a higher magnification in Figure 4(b). Only small fraction of transgranular cleavage being locally confined (not shown in Figure 4(b)) has been observed. Furthermore, a closer look at the fracture surface in Figure 4(b) reveals high density of pores. The origin of these pores i.e. whether they are formed under irradiation or during the mechanical testing is not known at the moment and requires additional investigations. The grains appear to be "coarsened" in comparison to the unirradiated state, see e.g. Figure 3(b). This is a consequence of dominant intergranular type fracture which makes three-dimensional grain morphology more pronounced, thus appearing them to be larger compared to flat fracture morphology (realizing due to predominantly transgranular cleavage observed in the unirradiated state at low test temperatures). Hence, explicit determination of the grain size by Electron Back Scatter Diffraction (EBSD) will be required to make an unambiguous conclusion. It has to be noted that EBSD study performed on the same IGP-W material after irradiation at 900 °C to 0.8 dpa did not reveal any significant grain growth compared to the unirradiated state [28].

Figure 4 (c), (d) show the fracture surface of the specimen tested at 1100°C. A stable crack growth with the characteristic dimple formation on the fracture surface is observed. This is in a good agreement with the reduction of the load beyond about 1 mm displacement, as reported in Figure 2(b). Although some of the dimples exhibit elongation (in the crack propagation direction), the overall morphology of the dimples does not show elongation, as it is observed in the unirradiated state in the case of ductile fracture, see Figure 3(d).

Figure 5 shows the HAADF-STEM micrograph from the FIB prepared lamella which was extracted from the irradiated specimen tested at 1050°C in the region close to the initial crack notch. High density of the dislocation tangles is observed, which is attributed to the under-tip plastic deformation occurred during extensive bending deformation of the specimen, as seen in Figure 2b. Irradiation induced needle-shaped precipitates with longitudinal dimensions of several hundreds of nm and disc-shaped precipitates up to 30 nm in diameter (not shown here) are also revealed. Furthermore irradiation induced voids with dimensions up to ~ 52 nm are mostly observed close to those precipitates and dislocation tangles. Dislocation loops could not be resolved for the given irradiation condition. In depth analysis of neutron irradiation induced alteration of microstructure in tungsten will be given in [29].

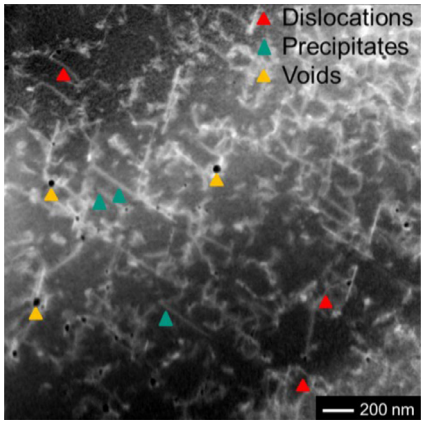

Figure 5. HAADF-STEM micrograph of the specimen irradiated to 1 dpa, 800 °C (WI06); STEM specimen is extracted from the deformed area of the fracture toughness specimen tested at 1050 °C. Markers point to an example of the dislocation lines/tangles, straight needle like precipitates, and voids.

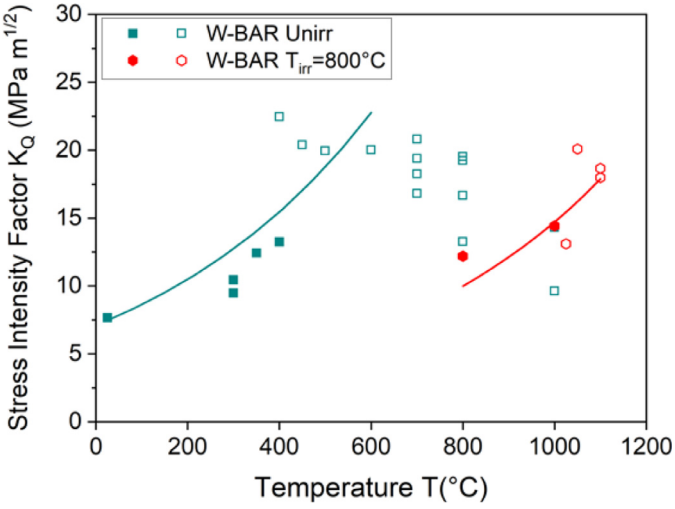

Figure 6. Fracture toughness of the IGP-W bar vs. temperature in the reference unirradiated state and after neutron irradiation. Values represented by open symbols do not satisfy the ASTM 399 validity criteria, see text. dK/dt = 0.6-0.7 MPa•m$^{1/2}$/s. The lines, $K_Q = 15.46 \cdot exp(0.00194 \cdot (T - 400))$ and $K_Q = 15.46 \cdot exp(0.00194 \cdot (T - 1025))$, guide the evolution of fracture toughness in the transition regions in the unirradiated and irradiated states, respectively.

4. Discussion

Conditional values of the fracture toughness (K_Q) vs. test temperature in the unirradiated state and after the neutron irradiation at 800°C are calculated from the load-displacement curves and are presented in Figure 6. Each data point represents a single fracture-mechanical test without averaging the results in the case of test duplication. The values satisfying ASTM E399 validity criteria (validity criterion on the maximum load the specimen is allowed to sustain and criterion on small scale yielding) are represented by solid symbols, while invalid data points are shown by open symbols. For the irradiated state, only the validity criterion on the maximum load the specimen is allowed to sustain was examined as the yield stress values are not known for the corresponding irradiated conditions. Generally, neutron irradiation is expected to increase the yield stress thereby relaxing the criterion on the small scale yielding. In the unirradiated condition, a steep increase of the K_Q values is seen at around 400°C. This is the lowest temperature where the non-linear load displacement behavior is observed (see Figure 2a). The latter is defined as the DBTT in the unirradiated state. Remarkably, the DBTT identified in this way is in a good agreement with the DBTT determined by Yin et al. [9] on the same material on the basis of flexural strain data. The solid cyan line shown in Figure 6 is a guide for the eye on the temperature evolution of K_Q in the transition region. Fitting the data points up to 600 °C with a Master Curve type function $K_Q = A + B \cdot exp(C \cdot (T - T_o))$, see e.g. [8], has been used to generate this guide line with A≥0, B>0, C>0 being the fitting parameters and with T_o being fixed to the DBTT value as determined above. Upon further increase in the test temperature, the validity criterion is no longer fulfilled due to the onset of the ductile deformation. Consequently, the fracture toughness values shown by open symbols represent a lower bound of the toughness, expected to be seen in sufficiently large size specimens satisfying the ASTM E399 validity criteria on the small scale yielding and on the maximum load, the specimen is allowed to sustain. The absence of reproducible stable crack growth at elevated temperatures prevents the application of ASTM E1820 procedure for the determination of K_{JC} [30] in the framework of elastic-plastic fracture mechanics. After the neutron irradiation at 800 °C to 1 dpa, the highest test temperature resulting in the valid fracture toughness shifts to 1000 °C. Above this temperature, extended inelastic deformation, as reported in Figure 2b, yields to invalid results. Taking into account the onset of non-linear load vs. displacement behaviour the DBTT can be estimated at 1000-1025 °C. This results the DBTT shift of 600-625 °C in comparison with the unirradiated state. The guide line in the irradiated state is obtained by an appropriate shift of T_o to 1025 °C.

In the case of the previously investigated polycrystalline rod [11] and round blank [8] tungsten products in equivalent specimen extraction orientations, predominantly intergranular fracture has been observed yielding the fracture toughness values between 7-9 MPa•m$^{1/2}$ at RT. It appears that in the case of current IGP-W, the chosen orientation for specimen extraction promotes a mixture of transgranular cleavage and intergranular fracture and results in a low fracture toughness being 8 MPa•m$^{1/2}$. This indicates that the fraction of the transgranular cleavage is still too low to enhance effective fracture toughness of the material. In the unirradiated condition, the brittle type fracture persists even above the DBTT though some isolated traces of the ductility have been recognized. This would indicate that grain boundary strength and material intrinsic fracture toughness, though substantially increased compared to low temperature values due to the increased load level at failure, are still too low to sustain the stable crack growth. The blunting of the crack tip due to absence of sharp fatigue precrack and subsequently due to low triaxiality may explain a delay in the crack initiation, however, it cannot explain why after the crack initiation, it may propagate either in a brittle or stable manner. Given the limited length of the ligament, the grain size and grain boundary character distribution might be responsible for the alternation of the deformation behaviour at and above 700 °C. Indeed, the anisotropy in the crystallographic texture found in the investigated material [9] may cause additional variation in the deformation behaviour. The neutron irradiation leads to the shift of the DBTT to higher temperatures indicating further weakening of the grain boundaries in comparison to the unirradiated state. The segregation of the trace impurities to the grain boundaries has been already proved for the unirradiated state; see for e.g. [11]. Correspondingly, no additional segregation of trace impurities to the grain boundaries is expected to take place under irradiation. A possible reason for the further weakening of the grain boundary may rather be the segregation/diffusion of transmutation elements Re and Os. This however requires dedicated investigations in the future. Furthermore, pores observed at grain boundaries, as presented in Figure 4, may also partly contribute to the weakening of the grain boundary strength. The TEM examination of the microstructure of the irradiated tungsten reveals a presence

of needle- (see Figure 5) and disc-shaped precipitates [29]. These were demonstrated to be W-Re intermetallic χ- and σ-phases, respectively [29]. These brittle intermetallic phases may act as crack initiation sites and thus should contribute to the embrittlement of the material in addition to the above-mentioned grain boundary weakening mechanisms. Furthermore, dislocation lines and tangles shown in Figure 5 are mostly observed close to the nm-sized precipitates and voids, indicating that these irradiation-induced features act as strong obstacles for dislocations movement. Hence, in addition to the formation of the intermetallic brittle phases and grain boundary segregation of transmuted elements, the suppression of the dislocation mobility by precipitates and voids is believed to be another important source of the material embrittlement. The change of the deformation behaviour in the irradiated state at 1025°C indicates an onset of the material ductility as supported by occasional observation of ductile crack growth. The blunting of the crack tip may be responsible for the absence of stable crack growth in the upper shelf (see Figure 2b). Finally, one needs to point out that the testing above irradiation temperature (800°C) may lead to a further evolution of the radiation damage by annealing and coarsening of the irradiation defects. Hence, the impact of the test temperature on the microstructural state has to be thoroughly studied in the future.

5. Summary

Fracture-mechanical properties of ITER specification stress-relieved IGP-W rod have been studied in the unirradiated reference state and after neutron irradiation at 800°C to 1 dpa. Linear-elastic fracture mechanics has been applied according to ASTM E399 for determination of quasi-static fracture toughness $K_{Q.}$ A brittle fracture dominated by transgranular cleavage has been found in the unirradiated state up to 600 °C. Qualitatively, various fracture behaviour (intergranular fracture, ductile crack growth, no failure) is observed at and above 700 °C which indicates a wide variation of notch triaxiality and distribution in grain boundary strengths. The blunting of the notch tip due to low triaxiality leads to a delay or complete suppression of the crack initiation above the DBTT. The latter explains the absence of the failure for some of the specimens up to severe deflection levels. After the crack initiation event, the differences between the observed brittle fracture and stable crack growth are attributed to the distribution of the grain boundary strengths and/or to the anisotropy in the texture. In the irradiated state, fracture mode is predominantly intergranular below the DBTT. Above the DBTT, crack initiation was either supressed due to low triaxiality of the notch or crack was emitted and grew stable leading to the characteristic dimple formation. The shift in the DBTT of 600-625 °C has been estimated on the basis of the onset on non-linear load vs. displacement behaviour. The observed DBTT shift is attributed to presence of the following irradiation effects (i) the formation of needle- and disk-shaped precipitates; (ii) segregation of the transmuted elements to the grain boundaries; and (iii) formation of voids. In addition, some fracture surfaces featured an evidence of grain coarsening, which needs further clarification and investigation by other experimental techniques. The large DBTT shift induced by the neutron irradiation should be accounted in the design process of tungsten-based PFC components.

Credit Author Statement

E. Gaganidze: Supervision, Investigation, Formal analysis, Writing - Original Draft, **A. Chauhan:** Investigation, Writing - Review & Editing, **H.-C. Schneider:** Investigation, Resources, Writing - Review & Editing **D. Terentyev:** Methodology, Resources, Writing - Review & Editing, **G. Borghmans:** Methodology, **J. Aktaa**: Writing - Review & Editing

Declaration of Competing Interest

The authors declare that they have no known competing financial interests or personal relationships that could have appeared to influence the work reported in this paper.

Acknowledgement

This work has been carried out within the framework of the EUROfusion Consortium and has received funding from the Euratom research and training programme 2014-2018 and 2019-2020 under grant agreement No. 633053. The views and opinions expressed herein do not necessarily reflect those of the European Commission.

We highly acknowledge Dr. Christian Dethloff for performing fractographic SEM study of the unirradiated fracture specimens. We thank S. Kohnle for preparation of unirradiated KLST specimens and carrying out the reference unirradiated fracture-mechanical tests. We highly acknowledge H. Ries for performing the fracture-mechanical tests in the Hot Cell of KIT's Fusion Materials Laboratory (FML). Valuable discussions with R. Rolli and his support regarding carrying out the post irradiation examination in FML is highly acknowledged.

References

[1] G. Federici, C. Bachmann, W. Biel, L. Boccaccini, S.Ciattaglia F.Cismondi, et al., Overview of the design approach and prioritization of R&D activities towards an EU DEMO, Fusion Engineering and Design 109-111 (2016) 1464–1474 Vols.
[2] H. Bolt, V. Barabash, W. Krauss, J. Linke, R. Neu, S. Suzuki, et al., Materials for the plasma-facing components of fusion reactors, Journal of Nuclear Materials 329-333 (2004) 66–73 Vols.
[3] M.R. Gilbert, J.-Ch. Sublet, Neutron-induced transmutation effects in W and W-alloys in a fusion environment, Nuclear Fusion 51 (2011) 043005.
[4] J.H. You, E. Visca, T. Barrett, B. Boeswirth, F. Crescenzi, F. Domptail, et al., European divertor target concepts for DEMO: Design rationales and high heat flux perfromance, Nuclear Materials and Energy 16 (2018) 1–11.
[5] A. Giannattasio, S.G. Roberts, Strain-rate dependence of the brittle-to-ductile transition temperature in tungsten, Philosophical Magazine 87 (2007) 2589–2598.
[6] D. Rupp, S.M. Weygand, Anisotropic fracture behaviour and brittle-to-ductile transition of polycrystalline tungsten, Philosophical Magazine 90 (2010) 4055–4069.
[7] B. Gludovatz, S. Wurster, A. Hoffmann, R. Pippan, Fracture toughness of polycrystalline tungsten alloys, Int. Journal of Refractory Metals and Hard Materials. 28 (2010) 674–678.
[8] E. Gaganidze, D. Rupp, J. Aktaa, Fracture behaviour of polycrystalline tungsten, Journal of Nuclear Materials 446 (2014) 240–245.
[9] C. Yin, D. Terentyev, T. Pardoen, R. Petrov, Z. Tong, Ductile to brittle transition in ITER specification tungsten assessed by combined fracture toughness and bending tests analysis, Materials Science & Engineering A 750 (2019) 20–30.
[10] A. Alfonso, D. Juul Jensen, G.-N. Luo, W. Pantleon, Recrystallization kinetics of warm-rolled tungsten in the temperature range 1150–1350°C, Journal of Nuclear Materials 445 (2014) 591–594.
[11] D. Rupp. *Bruch und Spröd-duktil-Übergang in polykristallinem Wolfram: Einfluss von Mikrostruktur und Lastrate.* Karlsruhe Institute of Technology, Dissertation 2010 : Shaker Verlag, 2010. Vol. 61. Schriftreihe "Werkstoffwissenschaft und Werkstofftechnik".
[12] ASTM E399 - 17. *Standard Test Method for Linear-Elastic Plane-Strain Fracture Toughness KIc of Metallic Materials.* s.l. : ASTM International, 100 Barr Harbor Drive, PO Box C700, West Conshohocken, PA 19428-2959. United States, 2017.
[13] T. Huu Loi, J.P. Morniroli, M. Gantois, Brittle fracture of polycrystalline tungsten, Journal of Materials Science 20 (1985) 199–206.
[14] B. Gludovatz, S. Wurster, T. Weingärtner, A. Hoffman, R. Pippan, Influence of impurities on fracture behaviour of tungsten, Philosophical Magazine 91 (2011) 3006–3020.
[15] T. Hirai, V. Barabash, F. Escourbiac, A. Durocher, L. Ferrand, V. Komarov, M. Merola, ITER divertor materials and manufacturing challenges. *Fusion Engineering and Design* 125 (2017) 250–255.
[16] T. Tanno, M. Fukuda, S. Nogami, A. Hasegawa, Microstructure Development in Neutron Irradiated Tungsten Alloys, Materials Transactions 52 (2011) 1447–1451.
[17] A. Hasegawa, M. Fukuda, K. Yabuuchi, Sh. Nogami, Neutron irradiation effects on the microstructural development of tungsten and tungsten alloys, Journal of Nuclear Materials 471 (2016) 175–183.
[18] X. Hu, T. Koyanagi, M. Fukuda, N.A.P. Kiran Kumar, L.L. Snead, B.D. Wirth, Y. Katoh, Irradiation hardening of pure tungsten exposed to neutron irradiation, Journal of Nuclear Materials 480 (2016) 235–243.

[19] J. Matejicek, J. Veverka, C. Yin, M. Vilemova, D. Terentyev, M. Wirtz, et al., Spark plasma sintered tungsten - mechanical properties, irradiation effects and thermal shock performance, Journal of Nuclear Materials 542 (2020) 152518.
[20] D. Terentyev, M. Vilemova, C. Yin, J. Veverka, A. Dubinko, J. Matejicek, Assessment of mechanical properties of SPS-produced tungsten including effect of neutron irradiation, International Journal of Refractory Metals and Hard Materials 89 (2020) 105207.
[21] I.V. Gorynin, V.A. Ignatov, V.V. Rybin, S.A. Fabritsiev, V.A. Kazakov, V.P. Chakin, V.A. Tsykanov, V.R. Barabash, Y.G. Prokofyev, Effects of neutron irradiation on properties of refractory metals, Journal of Nuclear Materials 191-194 (1992) 421–425 Vols.
[22] J. Habainy, Y. Dai, Y. Lee, S. Iyengar, Mechanical properties of tungsten irradiated with high-energy protons and spallation neutrons, Journal of Nuclear Materials 514 (2019) 189–195.
[23] M. Gorley, E. Diegele, E. Gaganidze, F. Gillemot, G. Pintsuk, Frank Schoofs, Ildiko Szenthe, The EUROfusion materials property handbook for DEMO in-vessel components—Status and the challenge to improve confidence level for engineering data, Fusion Engineering and Design 158 (2020) 111668.
[24] PLANSEE. The Plansee Group, www.plansee.com.
[25] M. Wirtz, J. Linke, Th. Loewenhoff, G. Pintsuk, I. Uytdenhouwen, Thermal shock tests to qualify different tungsten grades as plasma facing material, Phys. Scr. T167 (6pp) (2016) 014015.
[26] R.W. Margevicius, J. Riedle, P. Gumbsch, Fracture toughness of polycrystalline tungsten under mode I and mixed mode I:II loading, Materials Science and Engineering A270 (1999) 197–209.
[27] C. Yin, D. Terentyev, T. Zhang, R.H. Petrov, T. Pardoen, Impact of neutron irradiation on the strength and ductility of pure and ZrC reinforced tungsten grades, Journal of Nuclear Materials 537 (2020) 152226.
[28] D. Terentyev, et al. *SCK-CEN*.2020.
[29] A. Chauhan, Q. Yuan, E. Gaganidze, H.-C. Schneider, A. Brabaender, D. Terentyev, J. Aktaa, Microstructure characterization of the neutron irradiated ITER grade tungsten bar, paper under preparation, KIT (2020).
[30] ASTM E1820 - 18a. *Standard Test Method for Measurement of Fracture Toughness.* s.l. : ASTM International, 100 Barr Harbor Drive, PO Box C700, West Conshohocken, PA 19428-2959. United States, 2018.